BEST AVAILABLE IMAGES

Defective images within this document are accurate representations of the original documents submitted by the applicant.

Defects in the images may include (but are not limited to):

- BLACK BORDERS
- TEXT CUT OFF AT TOP, BOTTOM OR SIDES
- FADED TEXT
- ILLEGIBLE TEXT
- SKEWED/SLANTED IMAGES
- COLORED PHOTOS
- BLACK OR VERY BLACK AND WHITE DARK PHOTOS
- GRAY SCALE DOCUMENTS

IMAGES ARE BEST AVAILABLE COPY.

As rescanning documents *will not* correct images, please do not report the images to the Image Problem Mailbox.

Cell, Vol. 89, 309–319, April 18, 1997, Copyright ©1997 by Cell Press

Osteoprotegerin: A Novel Secreted Protein Involved in the Regulation of Bone Density

W. S. Simonet,[2] D. L. Lacey,[7] C. R. Dunstan,[7]
M. Kelley,[3] M.-S. Chang,[4] R. Lüthy,[4]
H. Q. Nguyen,[2] S. Wooden,[5] L. Bennett,[6]
T. Boone,[10] G. Shimamoto,[10] M. DeRose,[2]
R. Elliott,[1] A. Colombero,[1] H.-L. Tan,[7]
G. Trail,[5] J. Sullivan,[8] E. Davy,[3] N. Bucay,[2]
L. Renshaw-Gegg,[5] T. M. Hughes,[2] D. Hill,[7]
W. Pattison,[4] P. Campbell,[6] S. Sander,[5]
G. Van,[7] J. Tarpley,[7] P. Derby,[9] R. Lee,[10]
Amgen EST Program, and W. J. Boyle[1]
[1]Department of Cell Biology
[2]Department of Molecular Genetics
[3]Department of Protein Chemistry
[4]Department of Computational Biology
[5]Department of Mammalian Cell Molecular Biology
[6]Department of Immunology
[7]Department of Pathology
[8]Department of Bacterial Expression
[9]Department of Protein Structure
[10]Department of Process Science
Amgen Inc.
1840 DeHavilland Drive
Thousand Oaks, California 91320

Summary

A novel secreted glycoprotein that regulates bone resorption has been identified. The protein, termed Osteoprotegerin (OPG), is a novel member of the TNF receptor superfamily. In vivo, hepatic expression of OPG in transgenic mice results in a profound yet nonlethal osteopetrosis, coincident with a decrease in later stages of osteoclast differentiation. These same effects are observed upon administration of recombinant OPG into normal mice. In vitro, osteoclast differentiation from precursor cells is blocked in a dose-dependent manner by recombinant OPG. Furthermore, OPG blocks ovariectomy-associated bone loss in rats. These data show that OPG can act as a soluble factor in the regulation of bone mass and imply a utility for OPG in the treatment of osteoporosis associated with increased osteoclast activity.

Introduction

Bone is a complex tissue composed of cells, collagenous matrix, and inorganic elements. It provides many essential functions, including mechanical support, protection of vital organs, a microenvironment for hematopoiesis, and a depot for calcium and other minerals. The growth, development, and maintenance of bone is a highly regulated process (Nijweide et al., 1986). The level of bone mass reflects the balance of bone formation and resorption, which at the cellular level involves the coordinate regulation of bone-forming cells (osteoblasts) and bone-resorbing cells (osteoclasts). Osteoblasts arise from mesenchymal stem cells and produce bone matrix during development, after bone injury, and during normal bone remodeling that occurs throughout life. In contrast, osteoclasts differentiate from hematopoietic precursors of the monocyte–macrophage lineage and resorb bone matrix. Both these cell types are influenced by a wide variety of hormones, inflammatory mediators, and growth factors (Suda et al., 1992; Mundy, 1993a, 1993b). An imbalance of osteoblast and osteoclast functions can result in skeletal abnormalities characterized by increased (osteopetrosis) or decreased (osteoporosis) bone mass.

The study of osteopetrosis in mutant mice has led to significant advances in the understanding of the processes that regulate bone mass (Marks, 1989). From these studies we have learned the following: (i) genetic defects in osteoclast development, maturation, and/or activation lead to decreased bone resorption and uniformly result in severe osteopetrosis (Marks, 1989); (ii) the stromal microenvironment plays an essential role in osteoclast differentiation (Udagawa et al., 1989); (iii) signal transduction from the cell membrane through Src tyrosine kinase is necessary for osteoclast-mediated bone resorption (Soriano et al., 1991); and (iv) changes in gene expression patterns regulated by the nuclear factor Fos play an important role in osteoclast development (Wang et al., 1992; Grigoriades et al., 1994). Additionally, osteoclast maturation and activation are regulated by osteoblast-derived factors during remodeling (Rodan and Martin, 1981). The disregulation of osteoblast and osteoclast functions in these systems implicates genes that act as key determinants in the regulation of bone mass. However, relatively little is known about the soluble factors that act physiologically to regulate osteoclast development.

This report describes the isolation of a determinant in the regulation of bone mass, a novel secreted member of the tumor necrosis factor receptor (TNFR) superfamily. The TNFR superfamily consists mostly of transmembrane proteins that elicit signal transduction in a variety of cells. This novel member lacks any apparent cell-association signals, however, indicating it likely acts in the extracellular milieu. Transgenic mice expressing this secreted protein exhibit a generalized increase in bone density (osteopetrosis) associated with a decrease in osteoclasts. We named this protein Osteoprotegerin (OPG), i.e., to protect bone. Administration of recombinant OPG produces similar effects in normal mice and protects against ovariectomy-associated bone loss in rats. In vitro, OPG blocks osteoclastogenesis in a dose-dependent manner. OPG appears to block the differentiation of osteoclasts, the principal if not sole bone-resorbing cell type, suggesting that it can act as a humoral regulator of bone resorption.

Results

Identification and Isolation of a Novel Secreted TNFR-Related Protein

OPG was first identified by sequence homology as a possible novel member of the TNFR superfamily during a fetal rat intestine cDNA-sequencing project. A full-length version of this clone was isolated and sequenced

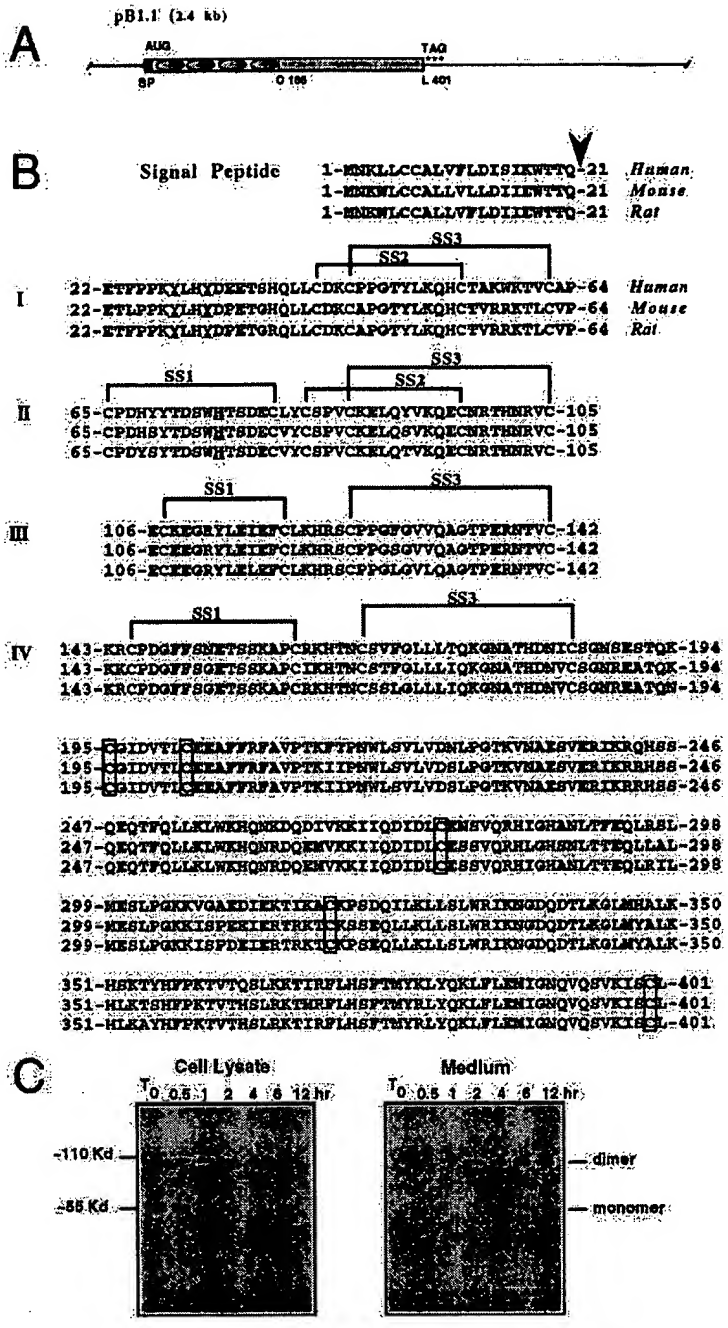

Figure 1. Osteoprotegerin Protein Structure and Secretion in Mammalian Cells

(A) Structure of the 2.4 kb rat intestinal pB1.1 clone indicating the position of the 401 aa open reading frame (bar). The closed box represents the 21-residue signal peptide, and shaded circles indicate the position of the 4 TNFR-like cysteine-rich domains.

(B) Alignment of human, mouse, and rat amino acid sequences. The location of the signal peptide cleavage site is indicated by a descending arrowhead. The four N-terminal TNFR-like cysteine-rich domains located between residues 22 and 194 are labeled I–IV. The predicted disulfide linkages (SS) for domains I–IV are indicated by bold lines. Either tyrosine 28 or 31 and histidine 75 (underlined) are predicted to form an ionic interaction. The cysteine residues located in the C-terminal half of OPG are boxed.

(C) Pulse-chase analysis of recombinant murine OPG produced in CHO cells. Cells were pulse-labeled for 30 min, then chased for the indicated time. Extracts of cells (left panel) and conditioned media (right panel) were immunoprecipitated, then analyzed by SDS–PAGE under nonreducing conditions. The relative mobility of the 55 kDa monomer and 110 kDa dimer are indicated.

(Figure 1A). This novel cDNA encodes a 401 amino acid (aa) polypeptide that has features of a secreted glycoprotein, such as a hydrophobic leader peptide, and 4 potential sites of N-linked glycosylation (Figure 1B). Although there were no existing matches in the database to the 401 aa reading frame, the predicted N-terminal half of the protein has a strong similarity to all members of the TNFR superfamily, most notably TNFR-2 and CD40. Unlike other known TNFR-like molecules, however, this protein contains no hydrophobic transmembrane-spanning sequence. The C-terminal half of OPG (aa 195–401) showed no homologies to any other known proteins nor contained any recognizable protein motifs. These data suggest that the rat *opg* cDNA encodes a novel secreted member of the TNFR family. Mouse and human *opg* cDNA clones isolated from normal kidney cDNA libraries also encode 401 aa proteins. The mouse and human proteins are ~85% and 94% identical to the predicted rat protein, respectively, indicating that the *opg* gene has been highly conserved throughout evolution (Figure 1B).

Pulse-chase labeling and immunoprecipitation of extracts obtained from OPG-transfected Chinese hamster ovary (CHO) cells show that OPG is a naturally secreted

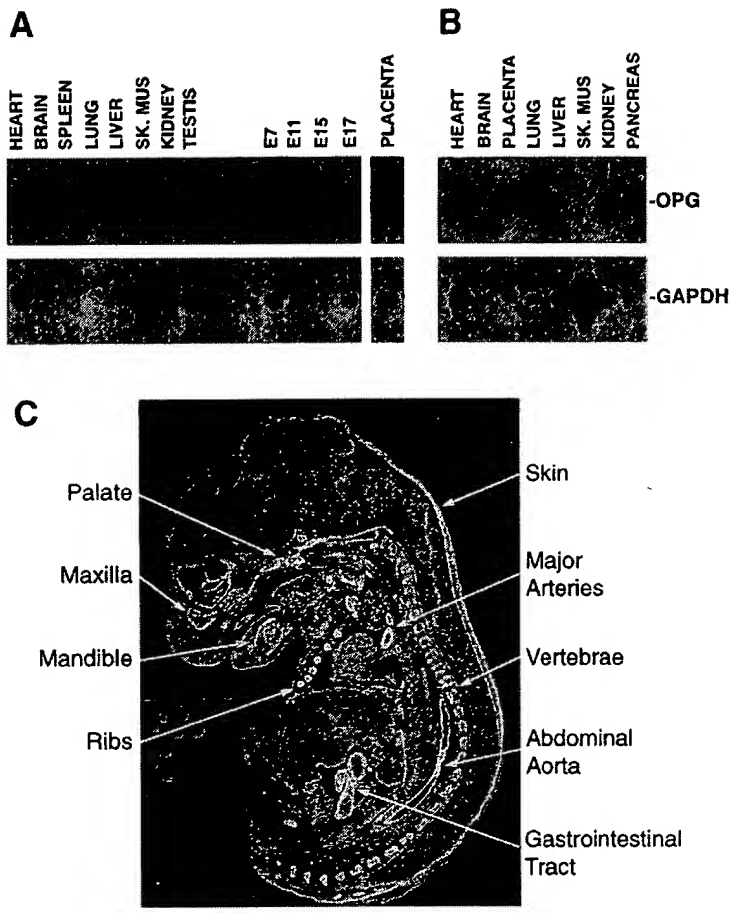

Figure 2. *opg* mRNA Expression in Tissues and during Mouse Embryogenesis

(A) Northern blot of poly(A)$^+$ mouse tissue or whole embryo RNA probed with a mouse *opg* cDNA probe (upper panel) or with a mouse *gapdh* cDNA probe (lower panel).

(B) Northern blot of poly(A)$^+$ human tissue RNA probed with a human *opg* cDNA probe (upper panel) or a mouse *gapdh* cDNA probe (lower panel). Both mouse and human OPG transcripts migrate as an approximately 3.0 kb band.

(C) In situ hybridization analysis of mouse *opg* mRNA expression in an E15 mouse embryo. Shown here is a saggital section of an E15 BDF1 mouse embryo that was hybridized overnight with [^{35}S]UTP antisense riboprobe for the detection of murine *opg* mRNA. Sense probe was used as a control and showed no signal (data not shown). Note the high expression of *opg* mRNA in cartilage rudiments of developing bones and in several major arteries, the gastrointestinal tract, and skin.

glycoprotein (Figure 1C). Initially, OPG is synthesized as an approximately 55 kDa monomer within the cell, is next converted to a disulfide-linked dimer of approximately 110 kDa, and is then secreted into the media (Figure 1C). While smaller amounts of monomeric OPG also are secreted, the predominant extracellular form of OPG is a disulfide-linked dimer. The monomeric and dimeric forms of OPG have been individually purified, and their N-terminal sequence has been determined (P. D., unpublished data). Both forms of OPG are cleaved during processing just before the glutamic acid residue at position 22 (Figure 1B), giving rise to a 380-residue mature protein. Under reducing conditions, OPG migrates as an approximately 55 kDa protein, larger than the 40 kDa predicted size of the mature polypeptide chain (data not shown). Upon treatment of purified OPG with N-glycanase, it migrates on reducing gels with an M_r of about 40 (M. K. and P. D., unpublished data), indicating that OPG is a glycoprotein. Together with the structural data described above, this suggests that OPG functions outside the cell as a secreted molecule capable of forming covalently bonded homodimers.

Patterns of OPG Expression in Mouse Tissues

opg transcripts of about 3.0 kb were detected by Northern blot hybridization in a number of murine tissues, including liver, lung, heart, and kidney (Figure 2A). *opg* mRNA is also expressed at high levels in the stomach, intestines, skin, and calvaria (data not shown). In human tissues, a transcript of similar size is detected at highest levels in the lung, heart, kidney, and placenta (Figure 2B), although there are detectable levels in various hematopoietic and immune organs (data not shown). During mouse embryonic development, *opg* transcripts are detected at high levels on day 7, whereas expression decreases at day 11 and then increases from day 15 to day 17 (Figure 2A). Since *opg* mRNA is expressed at relatively high levels in both mouse and human placenta, *opg* transcripts detected at day 7 may be due to the association of the placenta with the embryo at this developmental stage. Interestingly, there is a strikingly different pattern of OPG expression when comparing mouse and human tissues, most noticeably between brain, liver, and kidney. The reason for this is not clear, but it may reflect authentic differences in *opg* gene expression patterns between these two species. Alternatively, the levels of *opg* mRNA may physiologically vary, an aspect of this novel molecule that will need further study. Since OPG is a secreted protein, however, the site of its expression does not necessarily predict the site(s) at which it exerts its biological function.

Detection of *opg* mRNA transcripts by in situ hybridization in a day 15 mouse embryo is shown in Figure 2C. There is prominent expression of *opg* transcripts within the cartilagenous primordia of developing bone, most noticeably in the maxilla, mandible, the hyoid bone,

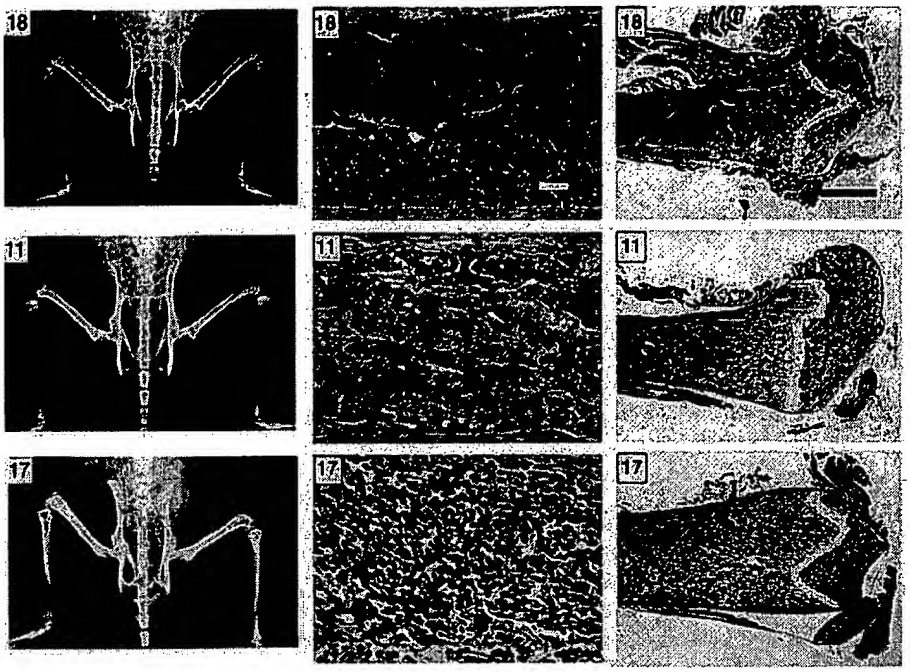

Figure 3. Increased Bone Density in *opg* Transgenic Mice

Two 10-week-old founder mice expressing relatively high (animal 17, bottom row) and low (animal 11, middle row) levels of *opg* transgene mRNA, and control littermate mouse (animal 18, top row) were subjected to X-ray (left column) or histologic (middle and right columns) analysis of their long bones, pelvis, and vertebrae. Increased bone density is seen in radiographs of transgenics 11 and 17, as are visible increases in bone by histological analysis. The lower power magnification (right column; bar = 1 mm) shows the distal femur and growth plate, and the higher power magnification (middle column; bar = 100 μm), shows the femoral midshaft. In these sections, bone stains deep blue or red, cartilage stains light blue, and marrow stains dark purple. Note the marbling effect reflecting the retention of cartilage remnants within trabeculae and the poorly defined cortex in the *opg* transgenics, particularly in animal 17 (lower middle and lower right panels, respectively). Increases in bone density are visible at birth in the high expressors and are detected with 100% penetrance in transgenic mice with elevated circulating levels of OPG.

the basiphenoid and basioccipital bones, the ribs, and the vertebrae. High expression was also detected in the brachiocephalic artery and ductus arteriosus, the left main bronchus, the abdominal aorta, and the midgut.

OPG Increases Bone Density In Vivo

To gain insights into the potential biological function for OPG, transgenic mice were generated that express the rat *opg* cDNA under the control of the human apolipoprotein E gene promoter and its associated liver-specific enhancer (Simonet et al., 1993). This vector has been previously used to generate mice containing high levels of secreted protein in their circulation (Simonet et al., 1994). Since OPG is a secreted receptor, any observable phenotype in mice overexpressing this protein should be the result of interactions with its cognate ligand, whether it is a soluble or a cell-surface protein. Five founder mice harboring the rat *opg* transgene were identified by Southern blot analysis of ear DNA samples and were analyzed at 8–10 weeks of age. Four of the five founders were found to express varying levels of transgene mRNA in their livers (data not shown). The rat OPG monomer and dimer were easily detectable in liver extracts and serum of high expressing transgenic mice but not control mice, indicating the transgene product was successfully delivered to the systemic circulation (W. S. S. and W. J. B., unpublished data).

The OPG-expressing animals and their normal littermates had no differences in external appearance, behavior, or bodyweight. Radiographs of intact animals showed a generalized increase in radiodensity of the long bones, vertebrae, and pelvis characteristic of osteopetrosis (Figure 3, left column). Despite this increase in radiodensity, there were no abnormalities in tooth eruption, which has been observed in other osteopetrotic mice (Yoshida et al., 1990; Soriano et al., 1991; Wang et al., 1992). Additionally, the relative size and shape of the bones in the expressors were not different from those of control mice. Upon gross dissection, splenomegaly was the only abnormality found in the transgene expressors. Analysis of organ weights indicated that only the spleens were increased (by ~38%) in the transgenic mice relative to controls. High expressors exhibited clear signs of osteopetrosis by radiography immediately following birth, with increasing severity throughout adolescence and adult life.

Histological analysis of bone sections from OPG expressors (Figure 3, founder animals 11 and 17) show severe osteopetrosis with the presence of trabeculae formed of bone-encased cartilage in the mid-diaphysis of the femur (Figure 3, middle column), a location normally

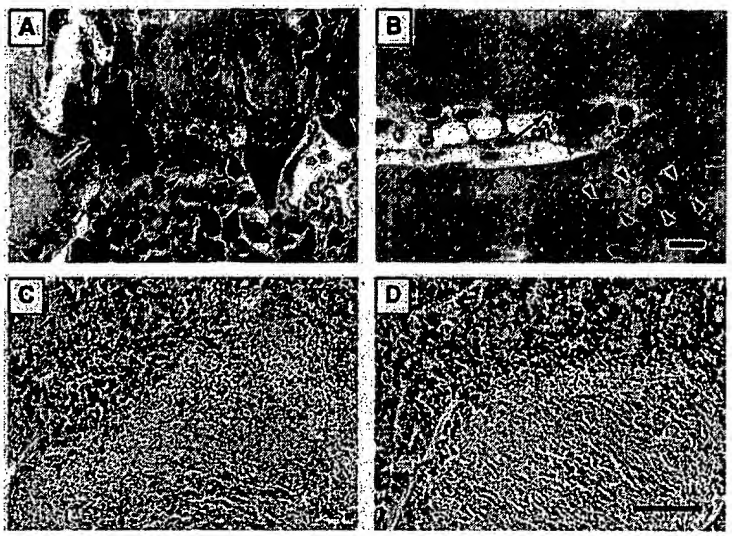

Figure 4. *opg* Transgenics Do Not Have a Defect in Monocyte–Macrophage Development but Appear to Have a Defect in Osteoclast Formation

Osteoclasts (arrows) in the distal femoral metaphysis were identified by TRAP cytochemistry. Many large multinucleated osteoclasts were present on the surface of metaphyseal trabecular bone in normal mice (A), while in the *opg* transgenic mice (B) only a few small TRAP-positive cells (possibly inactive osteoclasts) were seen in the same region. A cartilage remnant is marked "c," and its edge marked by arrowheads (bar = 10 μm). To confirm the presence of tissue macrophages, which share a common precursor with osteoclasts, immunohistochemistry was performed using anti-F480 antibodies, which recognize a cell-surface antigen on murine macrophages. The bottom panels are photomicrographs of spleens from either normal (C) or *opg* transgenic (D). Numerous F480-positive cells (brown staining) are detected in both spleens (bar = 100 μm). This is in marked contrast to what is observed in the osteopetrotic *Op* mice, which exhibit a defect in monocyte–macrophage development and a corresponding decrease in F480-positive cells in their spleens (Yoshida et al., 1990), suggesting that OPG is functioning to block osteoclast development at a more terminal step than the divergence of macrophage and osteoclast precursors.

filled by hematopoietic elements. The severity of the osteopetrosis correlated with the level of *opg* mRNA. In the highest expressors, a clearly defined cortex was not identifiable in sections of the femur (Figure 3, right column). Sections of vertebrae also show osteopetrotic changes, implying that the OPG-induced skeletal changes were systemic. Von Kossa staining of nondecalcified bone sections showed that the increased bone/cartilage matrix was mineralized (data not shown). Coincident with the loss of the marrow cavities, the spleens from the OPG expressors had an increased amount of red pulp, likely resulting from compensatory hematopoiesis owing to occlusion of marrow cavities with bone and cartilage. In addition to this, the highest OPG expressors had foci of extramedullary hematopoiesis within the liver (data not shown).

There were no other apparent gross pathologies in these mice, nor histologic abnormalities in the thymus, lymph nodes, gastrointestinal tract, pancreato-hepatobiliary tract, respiratory tract, reproductive system, genito-urinary system, skin, nervous system, heart and aorta, breast, skeletal muscle, or fat. These observations underscore the apparent skeletal selectivity of transgenically expressed *opg* activity.

The observed increase in bone density seen in *opg* transgenic mice could be due either to increased osteoblast synthesis of bone matrix or, conversely, to decreases in osteoclast-mediated bone resorption. The analysis of bone sections suggests that the latter process was affected. Based on H and E and tartrate-resistant acid phosphatase (TRAP) stains, the predominant difference in the expressors was the profound decrease in trabecular osteoclasts, both in the vertebrae and femurs (Figures 4A and 4B). This was particularly evident in the most severely affected animals. Similar to the severity of the osteopetrosis observed histologically, the magnitude of osteoclast deficiency correlated with the relative level of hepatic *opg* transgene mRNA. Circulating levels of OPG in these founder mice were not determined. However, F_1 transgenic progeny with radiographic and histological bone changes similar to founder mice 17 and 11 (Figure 3) had circulating OPG levels of 358 ± 79 and 14.2 ± 3.6 ng/ml (mean ± SD), respectively. Penetrance of the osteopetrotic phenotype was found to be 100% in mice with serum OPG levels greater than 10 ng/ml and varied in severity proportional to the level of systemic OPG. In contrast, OPG levels in the normal littermates were less than 2 ng/ml. (L. B., unpublished data).

The residual marrow present as islands within the osteosclerotic bone of high expressors showed predominantly myeloid elements. Megakaryocytes also were present at normal levels. Immunohistochemical staining of tissues for F480, a cell-surface antigen expressed by osteoclast precursors of the monocyte–macrophage lineage (Austyn and Gordon, 1981), showed the presence of positive cells in the marrow spaces and flattened directly adjacent to trabecular bone surfaces (data not shown). All hematopoietic elements and F480-positive cells were present in red pulp of both control and OPG mice (Figures 4C and 4D). In contrast, F480-positive cells are virtually absent in *Op* mutant mice, which carry a defective *csf-1* gene (Yoshida et al., 1990). The presence of F480-positive cells in *opg* transgenic mice rules out a generalized decrease in osteoclast precursors as the basis for the effects of OPG and suggests that OPG might regulate the terminal stages of osteoclast differentiation.

Recombinant OPG Blocks Osteoclastogenesis In Vitro

To determine whether or not OPG acts to regulate osteoclast differentiation, its effects were tested in an in vitro

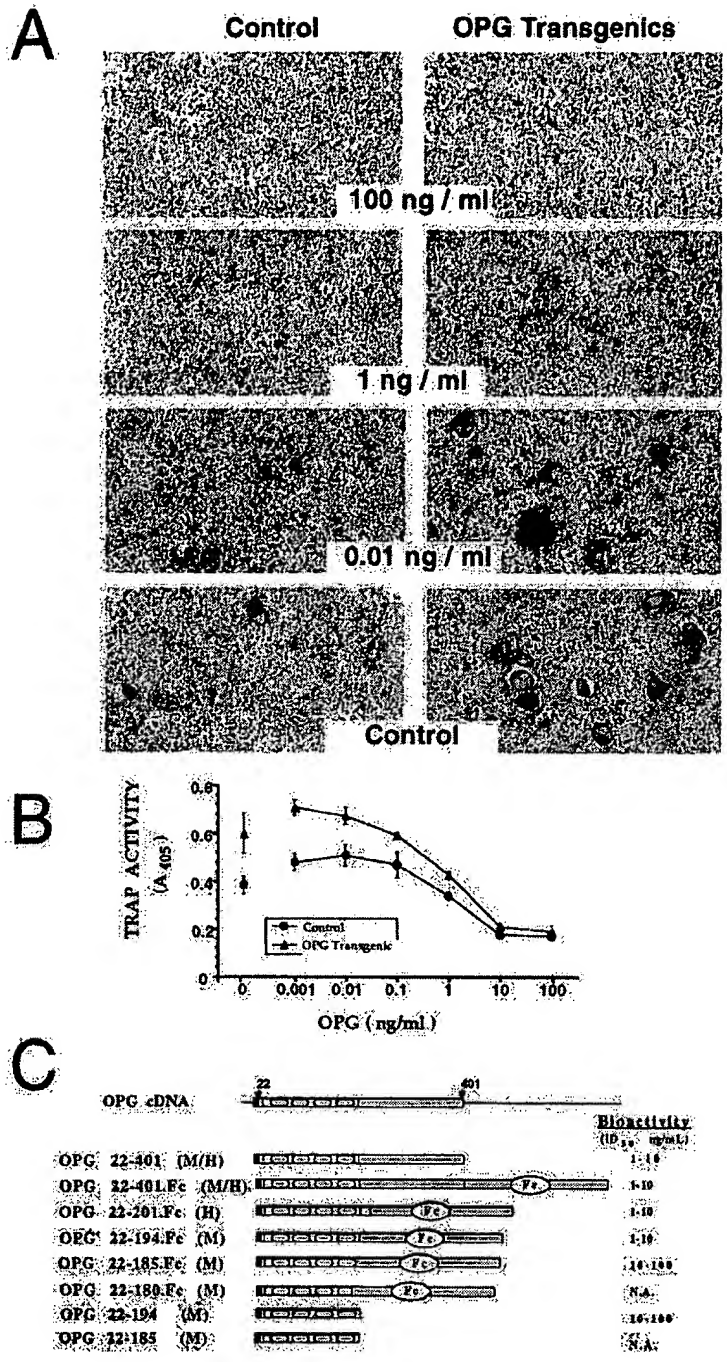

Figure 5. OPG Inhibits Osteoclastogenesis In Vitro

(A and B) Increasing concentrations of murine OPG [22–401]-Fc protein cause a dose-dependent decrease in the appearance of TRAP-positive osteoclasts (A) and TRAP activity (B) in osteoclast-forming cultures using splenocytes from either transgenic mice or their normal littermates (for assay details, see Experimental Procedures). Large multinucleated cells stained purple are mature osteoclasts. (B) shows the measurement of TRAP activity in treated cultures. Absorbance at 405 nm (A405) of lysed cultures plotted against OPG concentration indicates the conversion of p-nitrophenyl phosphate into p-nitophenol in the presence of sodium tartrate.

(C) Mapping the domain of OPG biological activity using the osteoclast-forming assay. Various constructs were used to make murine and human OPG-proteins of varying lengths. The construct length (left) and its relative bioactivity (right) are indicated. Bioactivity is expressed as the range in protein concentration (ng/ml) rendering half-maximal activity (ID_{50}). OPG proteins that are not active are indicated (N.A.). Note that truncation of the molecule proximal to cysteine residue 185, when fused to human Fc, led to a complete loss of biological activity.

osteoclast-forming assay (Lacey et al., 1995). This culture system allows maturation of osteoclasts from hematopoietic precursors that express multiple differentiation markers of the osteoclast lineage, most notably TRAP. Recombinant murine OPG fused to the human immunoglobulin IgG_1 Fc domain (murine OPG [22–401]-Fc) was purified from CHO cell-conditioned media and subsequently tested in the osteoclast-forming assay. In the absence of exogenous OPG, spleen cells from both the OPG-expressing mice and controls contained osteoclast precursors (Figure 5A), which confirms that there is no intrinsic defect in osteoclast development in OPG mice. At 100 and 10 ng/ml of the murine OPG, osteoclast formation from spleen cells of both control and OPG mice was completely inhibited (Figure 5A). The levels of TRAP were also inhibited in the presence of OPG, with an ID_{50} of about 1 ng/ml (Figure 5B). The levels of TRAP activity in culture lysates appeared to correlate with the

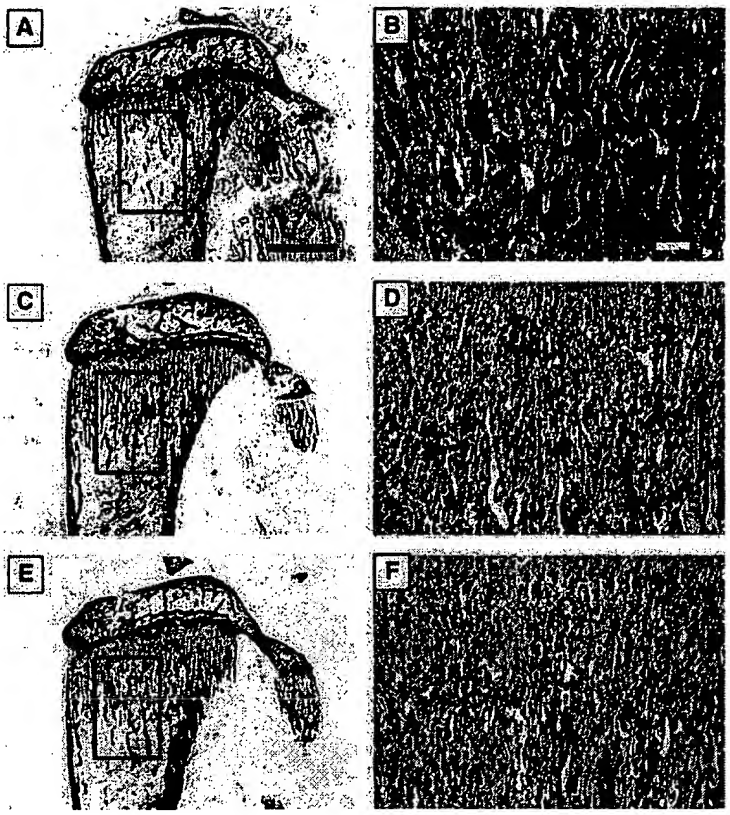

Figure 6. Recombinant OPG Administration Increases Bone Density in Normal Mice

Four-week-old male BDF1 mice (n = 5 per group) received subcutaneous injections of either vehicle (A and B), murine OPG [22–401]-Fc protein (10 mg/kg/day) (C and D), or the known antiresorptive pamidronate (5 mg/kg/day) (E and F) for seven days. The left panels are photomicrographs of Von Kossa-stained frozen sections of the proximal tibial metaphysis. Mineralized bone matrix is stained black in these micrographs, and shown is a similar visible increase in bone density in OPG-treated and pamidronate-treated mice relative to controls. Bone density was measured in the region highlighted (enclosed rectangles) and found to be increased in OPG and pamidronate-treated mice about 2- to 3-fold (see text). The right panels are photomicrographs of decalcified Masson's trichrome-stained sections of the distal femoral metaphysis of vehicle-treated (B), OPG-treated (D), or pamidronate-treated (F) mice. Development of a marbled appearance in the bone owing to cartilage retention in the OPG-treated (D) and pamidronate-treated (F) mice is similar to that seen in the high expressing founder 17 (see Figure 3). Bars in (A) and (B) indicate intervals of 1 mm and 100 μm, respectively.

relative number of osteoclasts seen by TRAP cytochemistry.

Additional forms of the human and murine OPG molecules were tested to determine portions of the protein required for biological activity (Figure 5C). Truncation of OPG N-terminal to cysteine 185 inactivates this molecule, presumably by disrupting the SS3 disulfide bond of the TNFR-like domain 4 (see Figure 1B). However, loss of the C-terminal portion of the molecule up to aa 194 did not affect activity. Thus, the N-terminal portion of OPG containing the TNFR-like domain is necessary and sufficient to inhibit osteoclastogenesis. All active forms of OPG inhibit osteoclastogenesis in a dose-dependent manner and possess half-maximal activities in the range observed for other potent cytokines in their respective in vitro assays (Figure 5C).

Recombinant OPG Increases Bone Density In Vivo

The transgenic model of OPG expression suggests that increases in bone and cartilage are due to elevated levels of circulating OPG. To prove this, OPG was administered to normal mice, and its effects on bone mass were measured and compared to the known antiresorptive bisphosphonate, pamidronate (Sietsema et al., 1989). Young rapidly growing mice (4 weeks of age) were subcutaneously injected daily with murine OPG [22–401]-Fc protein (10 mg/kg/day) or pamidronate (5 mg/kg/day). After 7 days, both the OPG and pamidronate recipients exhibited a marked increase in trabecular bone in the area of the tibial metaphysis relative to controls (Figure 6). A similar activity has been reported for this and other bisphosphonates (Sietsema et al., 1989). Based on histomorphometry of the proximal tibial metaphysis (Figures 6A, 6C, and 6E), the OPG-treated mice had an approximately 3-fold increase in trabecular bone compared to controls (31.1% ± 4.1% versus 12.0% ± 2.4%, respectively; mean ± SD, n = 5), which is highly significant ($p < 0.0001$). Pamidronate treatments also significantly increased trabecular bone volume (22.9% ± 0.6% over controls, $p < 0.001$). Administration of recombinant OPG or pamidronate also increased bone density in the metaphysis of the distal femur (Figures 6B, 6D, and 6F) and produced a pattern of cartilage retention within the bone trabeculae similar to that seen in transgenic founder 17 (Figure 3). In the OPG recipients, the serum level of OPG 24 hr after the last injection was 320 ± 176 ng/ml, a level similar to the steady-state levels in transgenic mice with a severe phenotype. Collectively, these data indicate that OPG acts as an antiresorptive agent that negatively regulates osteoclast maturation and can lead to the excess accumulation of newly synthesized bone and cartilage in vivo.

Recombinant OPG Protects Rats against Ovariectomy-Associated Bone Loss

A key test of the biological activity of OPG is to demonstrate that it can protect against pathological decreases of bone volume associated with loss of estrogen in ovariectomized rats. The ovariectomized rat is a commonly used animal model of human postmenopausal bone loss that is mediated by increased osteoclast activity (Christiansen et al., 1980; Kalu et al., 1989). Fisher rats, aged

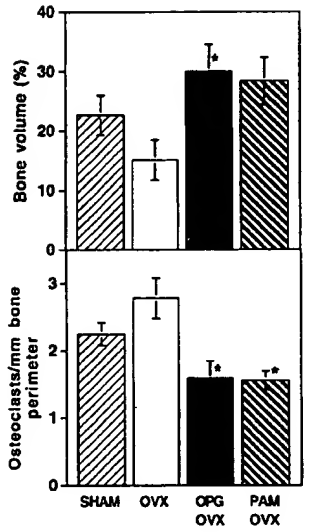

Figure 7. Recombinant OPG Blocks Ovariectomy-Induced Bone Loss in Fisher Rats

Twelve-week-old Fisher rats were ovariectomized and treated for 14 days with vehicle (OVX), murine OPG [22–401]-Fc protein (5 mg/kg/day) (OVX OPG), or pamidronate (5mg/kg/day) (OVX PAM). Sham-operated animals were treated with vehicle (SHAM). Bone volume in the proximal tibial metaphysis was increased in OPG OVX rats relative to OVX (upper panel, asterisk means different to ovariectomized animals, $p < 0.05$), and a similar trend is apparent in the SHAM and PAM OVX groups. Osteoclast numbers in the distal femoral metaphysis were decreased in the OPG OVX and PAM OVX relative to OVX (lower panel, asterisk means different to ovariectomized animals, $p < 0.05$).

12 weeks, were ovariectomized and after 4 days treated for 2 weeks with recombinant murine OPG [22–401]-Fc protein (5 mg/kg/day) or pamidronate (5 mg/kg/day). OPG-treated rats exhibited an increase in bone volume and a decrease in osteoclast numbers relative to controls (Figure 7). The known antiresorptive, i.e., pamidronate, had effects similar to OPG and those reported for other bisphosphonates (Wronski et al., 1989). These data show that OPG can act as a protective agent against inappropriately high rates of osteoclast-mediated bone resorption, in addition to its effects in normal animals.

Discussion

OPG is a novel secreted member of the TNFR superfamily, which inhibits osteoclast maturation and protects bone from both normal osteoclast remodeling and ovariectomy-associated bone loss. This protein contains two characterized domains: the N-terminal half, which harbors four tandem cysteine-rich TNFR motifs, and the C-terminal half, which is unrelated to any known protein sequences but appears to function in the association of OPG monomers as they are processed within the secretory pathway (W. J. B. and A. C., unpublished data). The TNFR superfamily consists primarily of transmembrane proteins that elicit signal transduction in a variety of cells and are known to mediate diverse biological responses, including cytotoxicity and apoptosis, and cell survival, proliferation, and differentiation (Smith et al., 1994). Soluble forms of these receptors have been identified and are generated either by cleavage from the cell membrane or as secreted molecules encoded by alternatively spliced mRNAs (Kohno et al., 1990; Hughes and Crispe, 1995). The soluble forms of these receptors are likely to capture and bind their cognate ligands, thereby preventing the ligands from activating their cellular targets. Several members of the Pox family of viruses express soluble TNF receptors, which aid in neutralizing the antiviral effects of TNFα (Smith et al., 1994; Schreiber et al., 1996). Interestingly, the only form of OPG that we have isolated is a secreted protein. Based on our analysis, we have not detected any qualitatively altered transcripts capable of encoding a transmembrane form of the protein.

Systemic delivery of OPG via the expression of rat or murine *opg* transgenes in mice results in severe yet nonlethal osteopetrosis. The osteopetrotic phenotype caused by OPG overexpression differs significantly from those observed in other mouse osteopetrotic models, whether generated by the disruption of specific genes (*src* or *fos* gene knockouts) or in naturally occurring mouse mutants (Marks, 1989; Yoshida et al., 1990). Osteopetrosis is often lethal in those models, and bone formation, as well as tooth eruption, are abnormal. *opg* transgenic mice are, in contrast, of normal size, have no apparent defects in tooth eruption, and have normally shaped bones. Histologically, the *opg* transgenic mice have a marked reduction in trabecular osteoclasts but no deficiency of osteoclast precursors, suggesting a defect in the later stages of osteoclast differentiation. *opg* transgenic mice do not appear to have any defects in the normal development of osteoclast progenitor cells, since osteoclast-like cells develop readily from in vitro cultures of *opg* transgenic spleen cells. Taken together, these findings suggest that OPG, and perhaps its ligand(s) or receptor(s), naturally serve to regulate bone density by modulating osteoclast differentiation from hematopoietic precursors.

Recombinant OPG protein inhibits osteoclast differentiation in a dose-dependent manner in an in vitro osteoclast-forming assay. The N-terminal 185 amino acids of OPG are required for activity, and truncations that disrupt the predicted SS3 bond of domain 4 eliminate activity. This suggests that the TNFR-related portion of OPG, which resembles the ligand-binding domain of other related receptors, is sufficient for arresting osteoclast maturation in vitro. One hypothesis for this activity is that OPG is neutralizing a TNF-related protein that normally acts as an osteoclast maturation factor. There are no known members of the TNF family that appear to possess this activity, although TNFα can induce bone resorption (Bertolini et al., 1986) and increase osteoclast formation in vitro (Thomson et al., 1987). It is noteworthy that TNF-binding protein, which does neutralize TNFα activity, fails to inhibit osteoclastogenesis in vitro and does not induce the accumulation of bone and cartilage in normal mice (D. L. L. and H.-L. T., unpublished data). Alternatively, OPG may bind to a TNF-related protein that acts as a receptor, a plausible theory since a majority of TNF family members are transmembrane proteins.

Several lines of evidence indicate that OPG may be

a key determinant regulating bone metabolism. First, overexpression in transgenic mice at a site distant to the bone results in a dramatic increase in bone density and inhibition of osteoclast maturation. The severity of the phenotype in the transgenics correlates with the levels of RNA expression in the liver and with circulating levels of protein. Second, OPG specifically inhibits osteoclastogenesis in vitro. Third, systemic administration of OPG produces an increase in bone density in the tibial metaphysis and blocks the loss of bone induced by ovariectomy. Fourth, in situ hybridization data indicate that the mouse gene is expressed at high levels in the cartilaginous primordia of bones throughout the fetus. Lastly, the human gene is localized to chromosome 8 q23–24, a region closely linked to the gene involved in hereditary multiple exocytoses (HME), a skeletal disorder resulting in bone malformation and, in some instances, chondrosarcoma (Ahn et al., 1995). This same locus harbors the gene for the bone morphogen BMP-1 (Tabas et al., 1991), a member of the TGFβ superfamily that has potent bone-forming activity in vivo, even in soft tissue sites away from bone. This raises the possibility that this region of chromosome 8 may harbor a gene cluster involved in the regulation of bone development and metabolism.

In summary, a novel member of the TNF receptor family has been identified, and its biological function deduced. Unlike other members of this family, Osteoprotegerin appears to function as a secreted protein. In addition, a novel gain-of-function model for nonlethal osteopetrosis has been generated by transgenic overexpression of OPG in mice. The phenotype of this model differs significantly from models generated by the targeted mutagenesis of the *src* and *fos* genes, and from naturally occurring mutant mouse strains, such as the *Op* mouse (CSF-1 disruption). Our analysis suggests that a step in osteoclast differentiation is impacted by OPG in vitro. Therefore, we propose that OPG is a secreted regulator of bone density that can act locally and systemically by negatively regulating osteoclast maturation. Our initial findings imply a utility for OPG in the treatment of osteopenic disorders that are characterized by excessive osteoclast activity, such as primary osteoporosis, Paget's disease of the bone, hypercalcemia of malignancy, and osteolytic metastases.

Experimental Procedures

Computational Biology

A cDNA library was constructed using mRNA isolated from rat embryonic d20 intestine for EST analysis (Adams et al., 1991). The resulting 5′ nucleotide sequence obtained from individual clones was translated and compared with the existing database of known protein sequences using a modified version of the FASTA program (Pearson, 1990). Analyses for the presence of specific protein motifs were carried out using a modified sequence profile (Lüthy et al., 1994).

A full-length *opg* cDNA clone containing a 2.4 kb insert (pB1.1) was isolated from a fetal rat intestine cDNA library by colony hybridization and sequenced. The mouse and human homologs of the rat *opg* cDNA were isolated from either mouse or human normal kidney cDNA libraries (Clontech, Palo Alto, CA) by PCR amplification and colony hybridization, then sequenced. A human DNA clone was obtained from a genomic P1 library (Genome Systems Inc., St. Louis, MO) by plaque hybridization with a labeled human *opg* cDNA probe and was used in fluorescence in situ hybridization (FISH) analysis to determine its chromosomal localization in metaphase chromosomes as described (Heng et al., 1992).

Expression and Analysis of Recombinant OPG Protein

Mouse and human OPG-Fc fusion protein vectors were constructed by PCR as previously described (Byrn et al., 1990) with minor modifications. The full-length *opg* reading frame was PCR amplified, then linked to glutamic acid residue 211 of the human IgG_1 Fc region through an artificial NotI adapter, creating the following junction sequence: KISCLAAAEPKSCD.

Variants of the human and mouse full-length OPG-Fc fusion proteins were constructed by PCR amplifying the OPG regions encoding residues 1–201 (human), 1–194 (mouse), 1–185 (mouse), and 1–180 (mouse), then fused to Fc as described above. The OPG-Fc chimeric sequences were then cloned into the plasmid vector pCEP4 (Invitrogen, San Diego, CA). The parent pCEP4 and pCEP4 OPG-Fc vectors were lipofected into 293-EBNA-1 cells (Invitrogen, San Diego, CA) and selected in 100 μg/ml hygromycin using the manufacturer's recommended methods. Serum-free media was produced, and the OPG-Fc fusion proteins were purified by protein A/G-affinity chromatography (Ey et al., 1978). The mouse and human *opg* cDNAs were also cloned into the eukaryotic expression vector pDSRα and expressed in stably transformed CHO cell lines as previously described (DeClerk et al., 1991). The purification of native recombinant OPG from CHO cell-conditioned media will be described in another publication (M. K. and E. D., unpublished data).

Rabbit polyclonal antibodies were raised to purified murine OPG [22–401]-Fc fusion protein by subcutaneous injection of antigen emulsified in adjuvant, then affinity purified. A CHO cell line overexpressing the murine OPG protein was metabolically labeled and immunoprecipitated as previously described (Boyle et al., 1991). In brief, subconfluent cultures were pulse-labeled with approximately 1.0 mCi/ml of [^{35}S]-Translabel (ICN, Irvine, CA) for 30 min, then chased with complete media for the indicated time interval. The conditioned media was removed and made 1% in NP-40 (v/v), and the cell monolayers were lysed with RIPA buffer. Both the media and cell lysates were clarified, then immunoprecipitated. Western blots of conditioned media and mouse serum samples were performed as previously described (Kamps and Sefton, 1988). The blots were probed with anti-OPG antibodies (0.1 μg/ml), and immune complexes detected by enhanced chemiluminescence (Amersham) after exposure to Kodak X-ray film.

mRNA Analysis

Northern blots of either total or poly(A)$^+$ mRNA were prepared as described (Jähner and Hunter, 1991) or purchased from a commercial source (MTN's, Clonetech, Palo Alto, CA). All blots were probed under stringent conditions with a ^{32}P-dCTP-labeled rat, mouse, or human *opg* DNA probe as indicated. These blots were subsequently probed with the mouse *gapdh* cDNA to verify the integrity of the blotted mRNA. Northern blot analysis was also performed on founder liver tissue RNA to assess the expression of the rat *opg* transgene.

In situ hybridization was performed on mouse embryos fixed in 4% paraformaldehyde. Antisense and sense RNA probes to murine OPG (bp 803–1000) were transcribed using viral RNA polymerases in the presence of [^{35}S]UTP from a PCR-generated template containing the T7 promoter. Embryo sections were hybridized with the appropriate probe, then covered with emulsion and exposed 2–3 weeks at 15°C. The slides were counter stained with methyl green prior to photography.

Generation of *opg* Transgenic Mice

The coding region for either the rat or murine *opg* cDNA was subcloned free of mutations into an expression vector placing it under the control of the human ApoE promoter and liver-specific enhancer element (Simonet et al., 1994). For microinjection, the ApoE-OPG plasmid was purified, and the transgene insert isolated. Single-cell embryos from BDF1 mice were injected essentially as described (Brinster et al., 1985) and cultured overnight in a CO_2 incubator. Fifteen to twenty 2-cell embryos were transferred to the oviducts of pseudopregnant CD1 female mice. Transgenic offspring were

identified by screening for the *ApoE-opg* transgene in DNA prepared from ear biopsies as described (Simonet et al., 1994).

Necroscopy and Pathological Analysis

At 8–10 weeks of age, 5 transgenic founder and 5 control animals were necropsied. Radiography was performed prior to the gross dissection. Bone tissue was decalcified using a formic acid solution, and all sections were stained with H and E. In addition, staining with Gomori's reticulin and Masson's trichrome was performed on certain tissues. To assess the status of matrix mineralization, frozen sections of nondecalcified bone were stained using the Von Kossa method. Using this method, the mineralized matrix is black, while other tissues stain red. Enzyme histochemistry was performed to determine the expression of TRAP. Immunohistochemistry for the monocyte–macrophage F480 surface antigen was also performed on formalin-fixed paraffin-embedded 4 μm sections using the rat monoclonal anti-mouse F480 antibody (Harlan, Indianapolis, IN). The antibody was detected by biotinylated rabbit anti-rat immunoglobulins and peroxidase-conjugated strepavidin (BioGenex, San Ramon, CA), using DAB as the chromagen (BioTek, Santa Barbara, CA). Immunohistochemistry sections were counterstained with hematoxylin.

In Vitro Osteoclast-Forming Assay

A cell-culture system allowing osteoclast development from hematopoietic precursor cells was used to analyze the effects of recombinant OPG (Udagawa et al., 1989; Lacey et al., 1995). Spleen cells were cultured in vitro overnight in alpha MEM containing 10% heat-inactivated fetal bovine serum supplemented with 500 U/ml CSF-1. After this incubation, the nonadherent cells were collected, subjected to gradient purification, and then cocultured with the bone marrow stromal cell line ST2 at a ratio of 1×10^5 ST2 cells to 1×10^6 nonadherent spleen cells/ml of media supplemented with dexamethasone (100 nM) and 1,25 dihydroxyvitamin D_3 (10 nM). Prostaglandin E_2 (250 nM) was added to some cultures to enhance osteoclast formation (Lacey et al., 1995). Cocultures were incubated for 8–10 days. New media containing fresh supplements was added every 3–4 days. Osteoclast formation was measured by quantitating the presence of TRAP using either cytochemical staining or by a TRAP-solution assay (Lacey et al., 1995). In the TRAP-solution assay, enzyme activity/well was measured by the conversion of p-nitrophenylphosphate (20 nM) to p-nitrophenol in the presence of 80 mM sodium tartrate and was expressed as optical density at 405 nm. To some cultures, recombinant OPG proteins were added at concentrations ranging from 0.001 ng/ml to 100 ng/ml during the coculture of nonadherent cells with ST2 cells. The half-maximal inhibitory dose (ng/ml) for OPG recombinant proteins (ID_{50}) was obtained semiquantitatively by extrapolating from the dose-response curves generated from OPG-treated cultures.

In Vivo Response to Recombinant OPG

Male BDF1 mice (Charles River, Wilmington, MA) aged 4 weeks were injected daily subcutaneously with recombinant murine OPG [22–401]-Fc fusion protein (10 mg/kg in phosphate-buffered saline), 5 mg/kg pamidronate ("Aredia," Ciba-Geigy, Tarrytown, NY), or carrier alone for 7 days (5 mice/group). On the day following the last injection, the mice were killed, blood was taken for the determination of circulating OPG levels, and the right tibia and femur were removed. The tibiae were frozen without decalcification, and longitudinal frozen sections cut through the midregion of the proximal metaphysis, using the fibula junction as a landmark. The sections were stained by Von Kossa stain to demonstrate mineralized bone and cartilage. Bone density was determined in a region 1×1.5 mm midway between the cortices adjacent to the edge of the growth plate by automated image analysis (Metamorph, Universal Imaging Systems, West Chester, PA). The femurs were decalcified and processed as described above.

Ovariectomized ($n = 22$) or sham-operated ($n = 10$) 12-week-old Fisher rats (Charles River, Wilmington, MA) were treated for 14 days with subcutaneous recombinant murine OPG [22–401]-Fc fusion protein in phosphate-buffered saline (5 mg/kg/day) or pamidronate (5 mg/kg/day), $n = 6$ per group. Sham-operated and 10 ovariectomized rats were treated with vehicle. The day following the last injection, rats were euthanized, and the right tibia and femur removed. Bone density was determined in frozen sections of the distal tibial metaphysis as described above. The femur was decalcified in formic acid, dehydrated, mounted, and stained with hematoxylin and eosin. Osteoclast numbers were determined in a region 1×0.6 mm proximal to the growth plate in the distal femoral metaphysis. Osteoclasts were identified microscopically based upon morphology and enumerated relative to bone perimeter with the aid of a digitizing platen and camera lucida. Measurements were analysed using Osteomeasure software (Osteometrics, Atlanta, GA). Statistical significance of results was evaluated by Dunnett's test to correct for multiple comparisons (JMP Statistical Software, SAS Institute, Cary, NC).

Acknowledgments

W. S. S., D. L. L., and C. R. D. made major contributions to this work. The Amgen EST Program is a large interdisciplinary group who collectively made significant contributions to this work. For more information on this group, please contact Sid Suggs (ssuggs@amgen.com). We thank Dr. Bob Bosselman for helpful suggestions and critical review of this manuscript and Dr. Lawrence M. Souza for his support and advice throughout all stages of this work.

Received February 13, 1997; revised March 6, 1997.

References

Adams, M.D., Kelley, J.M., Gocayne, J.D., Dubnick, M., Polymeropoulos, M.H., Xiao, H., Merril, C.R., Wu, A., Olde, B., Moreno, R.F., et al. (1991). Complementary DNA sequencing: expressed sequence tags and human genome project. Science *252*, 1651–1656.

Ahn, J., Lüdecke, J.-H., Lindow, S., Horton, W.A., Lee, B., Wagner, M.J., Horsthemke, B., and Wells, D.E. (1995). Cloning of the putative tumor supressor gene for hereditary multiple exostoses. Nature Genet. *11*, 137–143.

Austyn, J.M., and Gordon, S. (1981). F4/80, a monoclonal antibody directed specifically against the mouse macrophage. Eur. J. Immunol. *11*, 805–815.

Bertolini, D.R., Nedwin, G.E., Bringman, T.S., Smith, D.D., and Mundy, G.R. (1986). Stimulation of bone resorption and inhibition of bone formation in vitro by human tumor necrosis factor. Nature *319*, 516–518.

Boyle, W.J., Smeal, T., Defize, L.H.K., Angel, P., Woodgett, J.R., Karin, M., and Hunter, T. (1991). Activation of protein kinase C decreases phosphorylation of c-Jun at sites that negatively regulate its DNA-binding activity. Cell *64*, 573–584.

Brinster, R.L., Chen, H.Y., Trumbauer, M.E., Yagle, M.K., and Palmiter, R.D. (1985). Factors affecting the efficiency of introducing foreign DNA into mice by microinjecting eggs. Proc. Natl. Acad. Sci. USA *82*, 4438–4442.

Byrn, R.A., Mordenti, J., Lucas, C., Smith, D., Marsters, S.A., Johnson, J.S., Cossum, P., Chamow, S.M., Wurm, F.M., Gregory, T., Groopman, J.E., and Capon, D.J. (1990). Biological properties of a CD4 immunoadhesin. Nature *34*, 667–670.

Christiansen, C., Christensen, M.S., McNair, P., Hagen, C., Stocklund, K.E., and Transbol, I. (1980). Prevention of early postmenopausal bone loss: controlled 2-year study in 315 normal females. Eur. J. Clin. Invest. *10*, 273–279.

DeClerk, Y.A., Yean, T.-D., Lu, H.S., Ting, J., and Langley, K.E. (1991). Inhibition of autoproteolytic activation of interstitial procollagenase by recombinant metalloproteinase inhibitor MI/TIMP-2. J. Biol. Chem. *266*, 3893–3899.

Ey, P.L., Prowse, S.J., and Jenkin, C.R. (1978). Isolation of pure IgG1, IgG2a, and IgG2b immunoglobulins from mouse serum using protein A-Sepharose. Biochemistry *15*, 429–436.

Grigoriades, A.E., Wang, Z.Q., Cecchini, M.G., Hofstetter, W., Felix, R., Fleisch, H.A., and Wagner, E.F. (1994). c-Fos: a key regulator of osteoclast-macrophage lineage determination and bone remodeling. Science *266*, 443–448.

Heng, H.H.Q., Squire, J., and Tsui, L.-C. (1992). High resolution mapping of mammalian genes by in situ hybridization to free chromatin. Proc. Natl. Acad. Sci. USA *89*, 9509–9513.

Hughes, D.P.M., and Crispe, I.N. (1995). A naturally occuring soluble isoform of murine Fas generated by alternative splicing. J. Exp. Med. *182*, 1395–1401.

Jähner, D., and Hunter, T. (1991). The ras-related gene rhoB is an immediate-early gene inducible by v-Fps, epidermal growth factor, and platelet-derived growth factor in rat fibroblasts. Mol. Cell. Biol. *11*, 3682–3690.

Kalu, D.N., Liu, C.C., Hardin, R.R., and Hollis, B.W. (1989). The aged rat model of ovarian deficiency bone loss. Endocrinology *124*, 7–16.

Kamps, M.P., and Sefton, B.M. (1988). Identification of multiple novel polypeptide substrates of the v-src, v-yes, v-fps, v-ros, and v-erb-B oncogenic tyrosine protein kinases utilizing antisera against phosphotyrosine. Oncogene *2*, 305–315.

Kohno, T., Brewer, M.T., Baker, S.L., Schwartz, P.E., King, M.W., Hale, K.K., Squires, C.H., Thompson, R.C., and Vannice, J.L. (1990). A second tumor necrosis factor receptor gene can shed a naturally occuring tumor necrosis factor inhibitor. Proc. Natl. Acad. Sci. USA *87*, 8331–8335.

Lacey, D.L., Erdmann, J.M., Teitelbaum, S.L., Tan, H.-L., Ohara, J., and Shioi, A. (1995). Interleukin 4, interferon-γ, and prostaglandin E impact the osteoclastic cell-forming potential of murine bone marrow macrophages. Endocrinology *136*, 2367–2376.

Lüthy, R.I., Xenarios, I., and Bucher, P. (1994). Improving the sensitivity of the sequence profile method. Protein Sci. *3*, 139–146.

Marks, S.C., Jr. (1989). Osteoclast biology, lessons from mammalian mutations. Am. J. Med. Genet. *34*, 43–53.

Mundy, G.R. (1993a). Factors which stimulate bone growth in vivo. Growth Reg. *3*, 124–128.

Mundy, G.R. (1993b). Cytokines and local factors which affect osteoclast function. Int. J. Cell Clon. *10*, 215–222.

Nijweide, P.J., Burger, E.H., and Feyen, J.H.M. (1986). Cells of the bone: proliferation, differentiation and hormonal regulation. Physiol. Rev. *66*, 855–886.

Pearson, W.R. (1990). Rapid and sensitive sequence comparison with FASTP and FASTA. Meth. Enzymol. *183*, 63–98.

Rodan, G.A., and Martin, T.J. (1981). Role of osteoblasts in hormonal control of bone resorptions. A hypothesis. Calcif. Tissues Int. *33*, 349–351.

Schreiber, M., Rajarathnam, K., and McFadden, G. (1996). Myxoma virus T2 protein, a tumor necrosis factor (TNF) receptor homolog, is secreted by a monomer and dimer that each bind rabbit TNFα, but the dimer is a more potent TNF inhibitor. J. Biol. Chem. *271*, 13333–13341.

Sietsema, W.K., Ebetino, F.H., Salvagno, A.M., and Bevan, J.A. (1989). Antiresorptive dose-response relationships across three generations of bisphosphonates. Drugs Under Exp. Clin. Res. *15*, 389–396.

Simonet, W.S., Bucay, N., Lauer, S.J., and Taylor, J.M. (1993). A far-downstream hepatocyte-specific control region directs expression of the linked human apolipoprotein E and C-I genes in transgenic mice. J. Biol. Chem. *268*, 8221–8229.

Simonet, W.S., Hughes, T.M., Nguyen, H.Q., Trebaski, L.D., Danilenko, D.M., and Medlock, E.S. (1994). Long-term impaired neutrophil migration in mice overexpressing human interleukin-8. J. Clin. Invest. *94*, 1310–1319.

Smith, C.A., Farrah, T., and Goodwin, R.G. (1994). The TNF receptor superfamily of cellular and viral proteins: activation, costimulation, and death. Cell *76*, 959–962.

Soriano, P., Montgomery, C., Geske, R., and Bradley, A. (1991). Targeted disruption of the c-*src* proto-oncogene leads to osteopetrosis in mice. Cell *64*, 693–702.

Suda, T., Takahashi, N., and Martin, T.J. (1992). Modulation of osteoclast differentiation. Endocrine Rev. *13*, 66–80.

Tabas, J.A., Zasloff, M., Wasmuth, J.J., Emanuel, B.S., Altherr, M.R., McPherson, J.D., Wozney, J.M., and Kaplan, F.S. (1991). Bone morphogenetic protein: chromosomal localization of human genes for BMP1, BMP2A, and BMP3. Genomics *9*, 283–289.

Thomson, B.M., Mundy, G.R., and Chambers, T.J. (1987). Tumor necrosis factor α and β induce osteoblastic cells to stimulate osteoclastic bone resorption. J. Immunol. *138*, 775–779.

Udagawa, N., Takahashi, N., Akatsu, T., Sasaki, T., Yamaguchi, A., Kodama, H., Martin, T.J., and Suda, T. (1989). The bone marrow-derived stromal cells line MC3T3/PA6 and ST2 support osteoclast-like cell differentiation in cocultures with mouse spleen cells. Endocrinology *125*, 1805–1813.

Wang, Z.-Q., Ovitt, C., Grigoriadis, A.E., Möhle-Steinlein, U., Rüther, U., and Wagner, E.F. (1992). Bone and haematopoietic defects in mice lacking c-Fos. Nature *360*, 741–745.

Wronski, T.J., Dann, L.M., Scott, K.S., and Crooke, L.R. (1989). Endocrine and pharmacological suppressors of bone turnover protect against osteopenia in ovariectomized rats. Endocrinology *125*, 810–816.

Yoshida, H., Hayashi, S., Kunisada, T., Ogawa, M., Nishikawa, S., Okumura, H., Sudo, T., Shultz, L.D., and Nishikawa, S.-I. (1990). The murine mutation osteopetrosis is in the coding region of the macrophage colony stimulating factor gene. Nature *345*, 442–444.

GenBank Accession Numbers

The GenBank accession numbers for the rat, mouse, and human *opg* sequences reported here are U94330, U94331, and U94332, respectively.